AGU100 ADVANCING EARTH AND SPACE SCIENCE

Geophysical Research Letters

RESEARCH LETTER
10.1029/2019GL084021

On the Delayed Coupling Between Ocean and Atmosphere in Recent Weak El Niño Episodes

N. C. Johnson[1,2], M. L. L'Heureux[3], C.-H. Chang[4], and Z.-Z. Hu[3]

[1]Atmospheric and Oceanic Sciences Program, Princeton University, Princeton, NJ, USA, [2]NOAA Geophysical Fluid Dynamics Laboratory, Princeton, NJ, USA, [3]NOAA/NCEP Climate Prediction Center, College Park, MD, USA, [4]Center for Climate/Environment Change Prediction Research, Ewha Womans University, Seoul, South Korea

Key Points:
- Tropical Pacific zonal sea surface temperature gradients modulate tropical atmospheric patterns traditionally associated with El Niño
- An anomalously strong tropical Pacific zonal sea surface temperature gradient delayed the occurrence of recent weak El Niño events
- The zonal sea surface temperature gradient and associated atmospheric variables have strengthened significantly since 1979

Supporting Information:
- Supporting Information S1

Correspondence to:
N. C. Johnson,
nathaniel.johnson@noaa.gov

Citation:
Johnson, N. C., L'Heureux, M. L., Chang, C.-H., & Hu, Z.-Z. (2019). On the delayed coupling between ocean and atmosphere in recent weak El Niño episodes. *Geophysical Research Letters*, *46*, 11,416–11,425. https://doi.org/10.1029/2019GL084021

Received 6 JUN 2019
Accepted 11 SEP 2019
Accepted article online 10 OCT 2019
Published online 29 OCT 2019

Abstract The recent borderline El Niño events of 2014/2015 and 2018/2019 provided operational centers with unique challenges because of the apparent absence of typical coupling between the tropical atmosphere and ocean before onset. The mismatch between atmosphere and ocean raises questions about its causes and predictability. Here we analyze observational data since 1979 to show that a sea surface temperature pattern characterized by an anomalous gradient in the western and central equatorial Pacific played a critical role in inhibiting the expected onset of central tropical Pacific deep convection during these events. This sea surface temperature pattern, which produces an atmospheric response that opposes the response to elevated eastern Pacific sea surface temperatures, has become more prevalent over the past 40 years.

Plain Language Summary The El Niño–Southern Oscillation, a naturally occurring climate pattern that impacts most of the planet, develops through interactions between the tropical atmosphere and ocean. During the development of recent borderline El Niño episodes in 2014 and 2018, however, the tropical atmosphere failed to behave in a typical manner despite conducive oceanic conditions, providing forecasters with challenges in classifying the events and in forecasting their future development and global impacts. A key question is whether forecasters could have anticipated the atypical tropical atmospheric pattern or if it was the result of chaotic weather variability that could not have been forecast with much advance warning. Here we analyze 40 years of observational data and find that a sea surface temperature pattern in the western and central equatorial Pacific offsets the typical El Niño impacts during these events. This sea surface temperature pattern has become more prevalent over the past 40 years, which indicates a recent tendency for El Niño tropical atmospheric conditions to be weaker relative to past episodes. The identification of this characteristic sea surface temperature pattern provides hope that forecasters may be able to anticipate when it may reinforce or offset the atmospheric conditions associated with the El Niño–Southern Oscillation.

1. Introduction

The borderline El Niño events of 2014/2015 and 2018/2019 provided a unique challenge to forecasters because of the apparent mismatch between tropical atmospheric and oceanic conditions (McPhaden, 2015; Santoso et al., 2019). This mismatch generated uncertainty for operational centers regarding event classification and forecasting their potential impacts. The National Oceanic and Atmospheric Administration (NOAA) declares an El Niño Advisory (i.e., the occurrence of El Niño conditions) when the sea surface temperature (SST) anomaly (SSTA) in the Niño 3.4 region (5°S–5°N, 120°–170°W; the Niño 3.4 index hereafter) exceeds 0.5 °C, the anomaly is expected to exceed that threshold for at least five consecutive overlapping three-month seasons, and the tropical atmosphere exhibits clear evidence of coupling with the ocean in a way that is consistent with the dynamics of the El Niño–Southern Oscillation (ENSO). By boreal autumn in 2014 and in 2018, the Niño 3.4 index had reached the threshold for NOAA to declare an El Niño Advisory (see NOAA's official three-month running mean Niño 3.4 index, or Oceanic Niño Index, at www.cpc.ncep.noaa.gov/products/analysis_monitoring/ensostuff/ONI_v5.php), and both statistical and dynamical models had forecast a high probability of the Niño 3.4 index persisting above the 0.5 °C threshold for at least several seasons (see archived forecasts at https://iri.columbia.edu/our-expertise/climate/forecasts/enso/current/). Despite these positive indicators from the tropical ocean, and the actual persistence of the elevated SSTs in the eastern tropical Pacific, NOAA did not declare the occurrence of El Niño conditions until they became evident in February 2015 and January 2019, respectively, because tropical atmospheric conditions were not clearly consistent with El Niño before then.

One of the primary indicators of coupling considered by forecasters and the focus of this study is the pattern of anomalous tropical convection that accompanies SST anomalies in the Niño 3.4 region. During an El Niño episode, the Walker circulation weakens as the eastern edge of the western equatorial Pacific warm pool and the region of strongest deep convection expand eastward to the International Date Line, and sometimes farther east during stronger events (Johnson & Kosaka, 2016; Takahashi et al., 2011). These changes are critical for the ocean-atmosphere coupling that promotes further El Niño development (Gill & Rasmusson, 1983) and for the excitation of global atmospheric teleconnection patterns (Chiodi & Harrison, 2013; Trenberth et al., 1998). The expected eastward shift of deep convection was conspicuously absent in the boreal fall of 2014 and 2018 (as discussed more thoroughly in section 3.1).

The absence of this expected atmospheric response raises several questions. Was the atypical atmospheric pattern the result of the noise of climate variability primarily internal to the atmosphere, such as that of the Madden-Julian Oscillation? Given the weak amplitude of these recent events, it is plausible that the noise of internal atmospheric variability, with little predictability beyond a few weeks, overwhelmed the weak SST-forced atmospheric signal. Alternatively, did SST patterns independent of those we typically use to monitor ENSO interfere with the canonical tropical atmospheric El Niño pattern? If so, then the hope is elevated for potential skillful prediction of such a pattern on seasonal time scales. This possibility also would open other lines of inquiry, including whether dynamical forecast models can predict this pattern and the response to it. In addition, this viewpoint may indicate the importance of an SST pattern that is separate from the "central Pacific" (CP) and "eastern Pacific" (EP; e.g., Yu & Kao, 2007) ENSO types that dominate the ENSO "flavor" discussion, since both EP and CP El Niño types are expected to produce anomalously strong precipitation in the central equatorial Pacific (e.g., Ashok et al., 2007; Santoso et al., 2019).

Previous studies have focused on coupled ocean-atmosphere processes that regulated the SST evolution during El Niño events, including the sequence of events that limited the 2014 episode to a borderline event (Chiodi & Harrison, 2017; Hu & Fedorov, 2016; Levine & McPhaden, 2016; Menkes et al., 2014). In contrast with these studies, we instead focus on the reasons why the tropical atmosphere failed to manifest a typical atmospheric response despite tropical Pacific SSTAs reaching the threshold for El Niño. Specifically, we focus on the possible role of SST patterns in modulating the tropical atmospheric circulation over the central equatorial Pacific for a *given* Niño 3.4 index value. Through an analysis of observational data since 1979, we find that a zonal SST gradient pattern in the western and central tropical Pacific plays a significant role in modulating the atmospheric response to ENSO. We focus on the boreal autumn because this is the season when Niño 3.4 index first crossed the nominal threshold for El Niño during these weak events, providing unique challenges for monitoring and forecasting potential impacts, but we show that the basic findings apply to all other seasons as well. We also show that this modulation is related to statistically significant trends in Walker circulation strength and central tropical Pacific convection.

2. Data and Methods

2.1. Data

We analyze monthly tropical observational data covering the period of 1979–2018. The SST data are from the Extended Reconstructed SST version 5 (Huang et al., 2017). We focus on Extended Reconstructed SST version 5 because of its prominent role in NOAA's ENSO monitoring, but we also carried out all analyses with Hadley Centre Sea Ice and SST version 1 data set (Rayner et al., 2003). All conclusions are insensitive to SST data set, and we do not discuss the Hadley Centre Sea Ice and SST version 1 results further except in the context of trends in section 3.2. As a proxy for tropical deep convection, we use outgoing longwave radiation (OLR) data available from the University of Maryland OLR Climate Data Record website (Lee et al., 2007). We calculate anomalies by removing the calendar month means. For OLR, we use a base period of 1981–2010. For SST, we follow the procedure used by the NOAA Climate Prediction Center for real-time ENSO monitoring and use centered 30-year base periods updated every five years (e.g., 1981–1985 anomalies use a 1966–1995 base period). The Climate Prediction Center adopted this procedure to counter the influence of long-term trends that do not reflect interannual variability in ENSO monitoring, but as discussed in the section 3.2, multidecadal trends still have a significant influence on the relationship between the Niño 3.4 index and the tropical atmosphere.

We also analyze relationships between ENSO and the Walker circulation strength, as measured by the Equatorial Southern Oscillation Index (EQSOI) derived from reanalysis data. The EQSOI is calculated as the normalized difference between the standardized sea level pressure anomalies averaged between the eastern equatorial Pacific (5°S–5°N, 80°W–130°W) and the equatorial region centered on Indonesia (5°S–5°N, 90°E–140°E). Anomalies are calculated with respect to the 1981–2010 base period. To sample the uncertainty associated with the choice of reanalysis data set, we consider the EQSOI derived from the European Centre for Medium-Range Forecasts ERA-Interim Reanalysis (Dee et al., 2011), National Centers for Environmental Prediction–Department of Energy Reanalysis 2 (Kanamitsu et al., 2002), National Centers for Environmental Prediction/National Center for Atmospheric Research Reanalysis (CDAS; Kalnay et al., 1996), and the Climate Forecast System Reanalysis (Saha et al., 2010). For analyzing the relationship between tropical SST indexes and the spatial pattern of anomalous low-level wind, we use gridded National Centers for Environmental Prediction/National Center for Atmospheric Research reanalysis 850-hPa wind data.

2.2. Methods

Our analysis focuses on the use of least squares linear regression to diagnose the boreal autumn (September–November (SON)) relationship between the central tropical Pacific OLR and ENSO, as monitored by the Niño 3.4 index, and between the central tropical Pacific OLR and SSTs independent of the Niño 3.4 index. We define a central Pacific OLR index (OLR_{DL}) as the area-averaged OLR anomaly for the equatorial region centered on the Date Line (5°S–5°N, 160°E–160°W), a key action center for anomalous deep convection associated with ENSO (e.g., Deser & Wallace, 1990; Johnson & Kosaka, 2016). We also considered the central Pacific OLR (CP-OLR) index of L'Heureux et al. (2015), which is based on a box average farther east (5°S–5°N, 170°E–140°W), but we choose a box centered slightly west of this region because the relationship between the Niño 3.4 index and OLR is more linear near the Date Line. However, the conclusions are insensitive to the focus on OLR_{DL} or CP-OLR indexes.

In this study, we seek to determine if a second predictor independent of the Niño 3.4 index, either a second SST index or the long-term trend, has a significant influence on OLR_{DL}. For this assessment, we compare linear regression models and determine the significance of the second predictor with an F test, for which an effective sample size accounts for autocorrelation following Santer et al. (2000). The null hypothesis is rejected; that is, the addition of a second predictor is significant, if F is greater than the critical value of the F distribution for a false rejection probability of 5% (see Text S1 for more details).

3. Results

3.1. Relationship Between Niño 3.4 Index and OLR_{DL}

We first focus on the relationship between the Niño 3.4 index and OLR_{DL} in SON, with an emphasis on the recent weak El Niño episodes of 2014 and 2018. In Figure 1, we show the SON OLR and SSTA patterns in 2014 (Figure 1a) and 2018 (Figure 1b), as well as the scatterplot between SON OLR_{DL} and the Niño 3.4 index from 1979 through 2018 (Figure 1c). As discussed in section 1, despite positive SSTAs in the eastern and central equatorial Pacific, the Pacific OLR anomaly patterns in the boreal fall of 2014 and 2018 did not resemble that of the canonical El Niño. Most notably, both years lacked the typical El Niño east-west OLR dipole, with positive OLR anomalies centered over Indonesia and negative OLR anomalies centered near the Date Line (see Figure 3a).

Overall, the relationship between SON OLR_{DL} and the Niño 3.4 index (Figure 1c) is strong ($r = -0.92$); however, the deviations from this linear relationship are large enough that the sign of OLR_{DL} can deviate from the expected ENSO relationship for weak events. Indeed, both 2014 and 2018 had positive SON OLR_{DL} anomalies, which contrasts the expected negative anomalies for El Niño conditions (Figure 1c).

Are these OLR_{DL} deviations from the linear Niño 3.4 relationship attributable solely to internal atmospheric variability, or do slowly varying and potentially more predictable SST variations also play a role? To begin to address this question, we follow a procedure similar to partial least squares regression analysis (Black et al., 2017; Smoliak et al., 2010; Wold, 1966) by first linearly removing the influence of the Niño 3.4 index

10.1029/2019GL084021

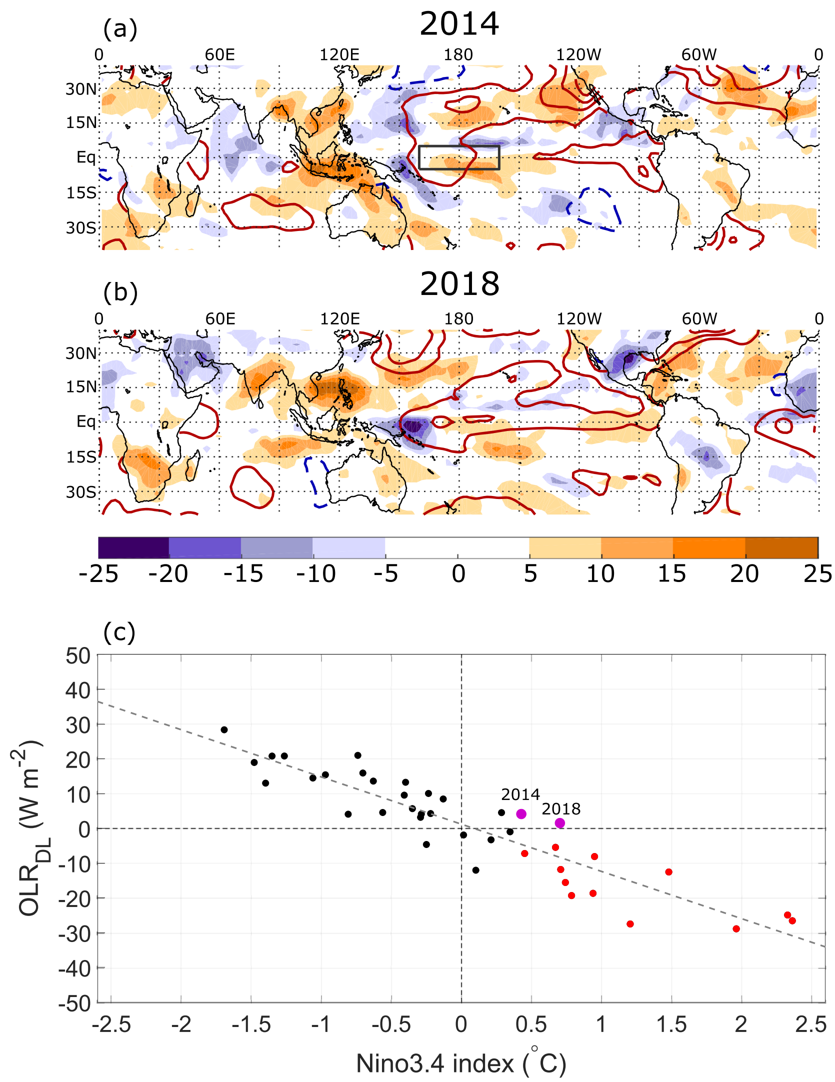

Figure 1. The relationship between boreal autumn central Pacific OLR and SSTs during El Nino episodes. The top two panels show the SON SST (°C; contours) and OLR (W/m^2; color shading) anomalies during the weak El Niño episodes of (a) 2014 and (b) 2018. SST is contoured at intervals of 0.5 °C with solid red and dashed blue contours indicating positive and negative anomalies, respectively, and the zero contour is omitted. The gray box centered on the Date Line in (a) represents the area that defines OLR_{DL}. (c) Scatterplot of OLR_{DL} and Niño 3.4 index for all autumns (SON) from 1979 to 2018. Red dots indicate all years that developed into El Niño by the end of winter according to the NOAA CPC criteria, excluding 2014 and 2018. The 2014 and 2018 cases are shown as purple dots. The dashed gray line represents the least squares linear fit.

from the SON OLR_{DL} time series and the gridded SSTA time series. We then correlate the residual OLR_{DL} time series with the residual SSTA fields. The resulting correlation map (Figure 2) indeed reveals a strong relationship, with correlations exceeding 0.7 north of Papua New Guinea and negative correlations below −0.4 at the equator around 150°W. This finding indicates that SST variability separate from that of the Niño 3.4 index contributes a substantial fraction of the OLR_{DL} variability. The correlation maps for the other seasons (Figure S1) show differences over regions such as the eastern equatorial Pacific, but for all seasons we see positive correlations near Papua New Guinea and negative correlations somewhere between 150°W and 180°W.

An elevated Niño 3.4 index typically indicates a weakening of the zonal tropical SST gradient and an eastward extension of the warm pool toward the Date Line, which is responsible for the anomalous Date Line convection and subsequent unstable air-sea interaction (Clarke, 2014; Gill & Rasmusson, 1983;

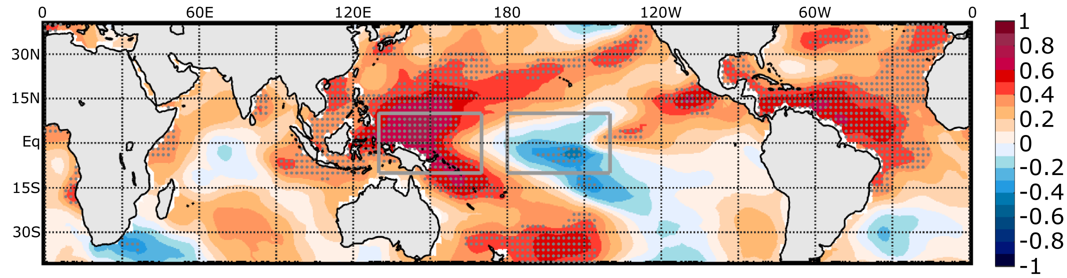

Figure 2. The influence of SSTs independent of the Niño 3.4 index on central Pacific convection. The correlation between the residual (i.e., Niño 3.4 index linearly removed) OLR_{DL} and SSTAs in SON. Gray stippling indicates regions where the partial correlation coefficients are statistically significant at the 5% level based on an F test. The gray boxes indicate the regions used to define a zonal SST gradient index, as described in the text.

Shu & Clarke, 2002). Figure 2 indicates, however, that this Niño 3.4 index influence can be counteracted by an anomalously strong SST gradient between ~150°E and 150°W. The physical justification is that elevated SSTs near Papua New Guinea and suppressed SSTs near and east of the Date Line potentially can prevent the eastward extension of the eastern edge of the warm pool that typically accompanies elevated Niño 3.4 index values. Therefore, the warmest Indo-Pacific warm pool waters, which anchor the heaviest tropical Pacific rainfall, may remain near Indonesia and away from the Date Line even when the Niño 3.4 index crosses the threshold necessary for an El Niño event to be declared.

To quantify the influence of the anomalous western/central equatorial Pacific SST gradient, independent of the Niño 3.4 index, on boreal autumn central Pacific convection, we first define a *zonal SST gradient index* (gradient index hereafter) as the difference between the standardized SSTA averaged over a box near Papua New Guinea (10°S–10°N, 130°E–170°E) and the standardized SSTA averaged over a box in the central Pacific (10°S–10°N, 180°–140°W). These boxes are chosen based on the strongest correlations in Figure 2 and on the physical justification described above.

To evaluate the role of the potentially competing influences of the gradient and Niño 3.4 indexes, we next quantify the impact of both the Niño 3.4 index and the linearly independent contribution from the gradient index on the SON tropical OLR and 850-hPa wind fields. For the latter calculations, we first linearly remove the Niño 3.4 index from both the gradient index (which we call the residual index) and the gridded OLR and wind anomaly fields. To facilitate a direct comparison between the Niño 3.4 and gradient index contributions, we standardize the Niño 3.4 and *residual* gradient indexes prior to regressions with the OLR and wind anomaly fields (Figures 3a and 3b). Both the unfiltered and residual OLR_{DL} and gradient index time series are illustrated in Figures S2 and S3. The OLR anomaly contribution from the Niño 3.4 index (Figure 3a) provides the familiar east-west dipole, with suppressed convection (positive OLR anomalies) over the maritime continent, and enhanced convection (negative OLR anomalies) centered near the Date Line. The 850-hPa wind regression also provides a familiar pattern (e.g., Deser & Wallace, 1990), with anomalous equatorial westerlies, signifying a weakened Walker circulation.

The gradient index contribution (Figure 3b) is nearly opposite to that of the Niño 3.4 index influence, with suppressed convection over the Date Line, as expected, and anomalous equatorial easterlies in the central Pacific. Note that the contour interval is halved in Figure 3b, which indicates that the Niño 3.4 index influence generally is stronger. This largely reflects the much stronger variance of the Niño 3.4 index (prior to standardization) relative to the residual gradient index. However, in years like 2018 when the Niño 3.4 SSTA is relatively modest (standardized value of 0.67) in relation to the gradient index (standardized residual index value of 1.86), then the two predictors can have an effect of similar strength.

This point is illustrated clearly in the time series of observed and linearly regressed OLR_{DL} anomalies (Figure 3c). The linear regression with both the Niño 3.4 and gradient indexes as predictors captures the OLR_{DL} variability more accurately ($R^2 = 0.93$; r between the residual OLR_{DL} and residual gradient index is 0.76) than with the Niño 3.4 index alone ($R^2 = 0.84$); the SST gradient predictor is highly significant (p value $<10^{-4}$) according to an F test. Table S1 indicates that the SST gradient index is a significant predictor at the 5% level for all other seasons as well. Notably, the inclusion of the gradient index as a predictor

10.1029/2019GL084021

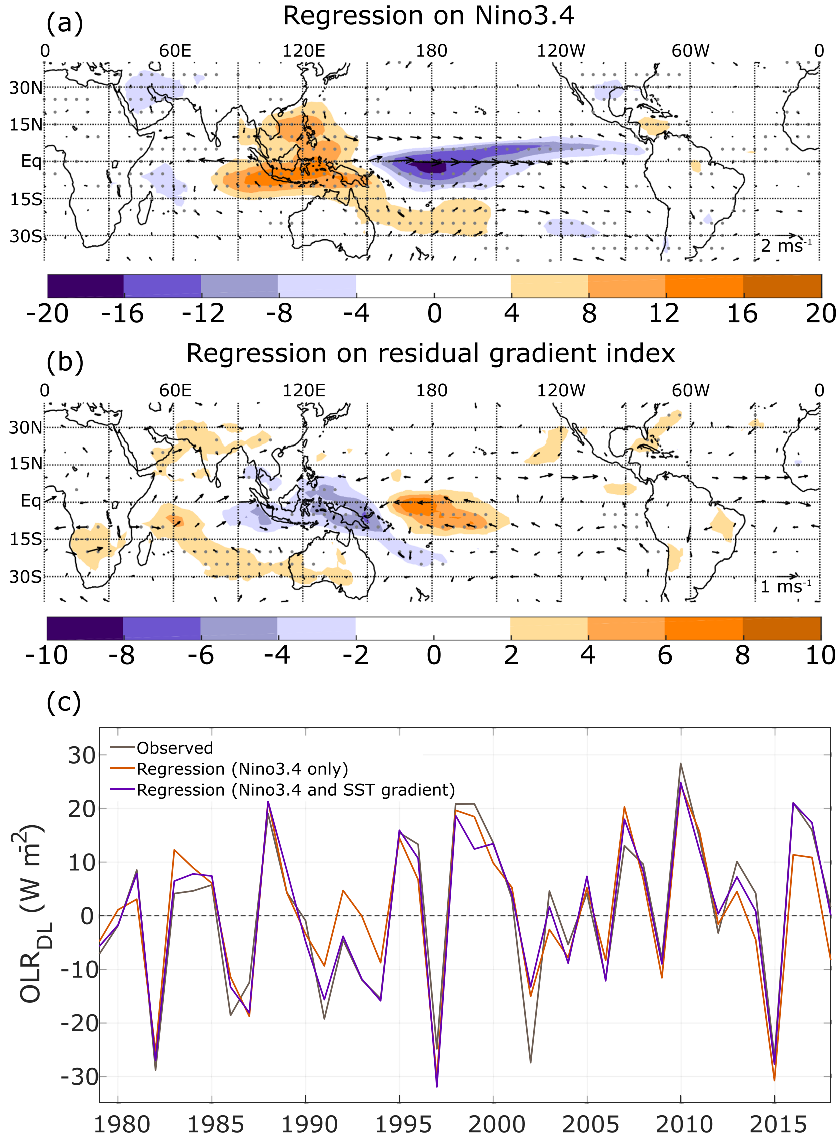

Figure 3. Linear regression of boreal autumn OLR and 850-hPa wind on tropical SST indexes. The top two panels show the gridded SON OLR (color shading; W/m^2) and 850-hPa wind (arrows; m/s) anomalies regressed on the (a) standardized Niño 3.4 and (b) standardized residual zonal SST gradient index. Gray stippling indicates where the OLR regression coefficients are significant at the 5% level based on an *F* test. The bottom panel (c) shows the following time series of SON OLR_{DL} anomalies: (gray) observations, (orange) linear regression with the Niño 3.4 index as the only predictor, and (purple) linear regression with both the Niño 3.4 and SST gradient indexes as predictors.

captures the near-zero OLR_{DL} values in the borderline El Niño events of 2014 and 2018, which means that a stronger-than-normal zonal SST gradient index countered the influence of the elevated Niño 3.4 index. Returning to the questions posed in the introduction, we conclude that an SST pattern independent of the Niño 3.4 index played a critical role in the absence of the typical atmospheric response for recent borderline El Niño events, including SON 2018.

3.2. Linear Trends of the Tropical Atmosphere

Close inspection of Figure 3c indicates that the linear regression of OLR_{DL} on the Niño 3.4 index alone (orange line) tends to overestimate OLR_{DL} early in the period and underestimate it late in the period. This visual impression is substantiated by a statistically significant downward trend in the difference between the observed and Niño 3.4-only regression lines (Figure S4). This suggests that the influence of the

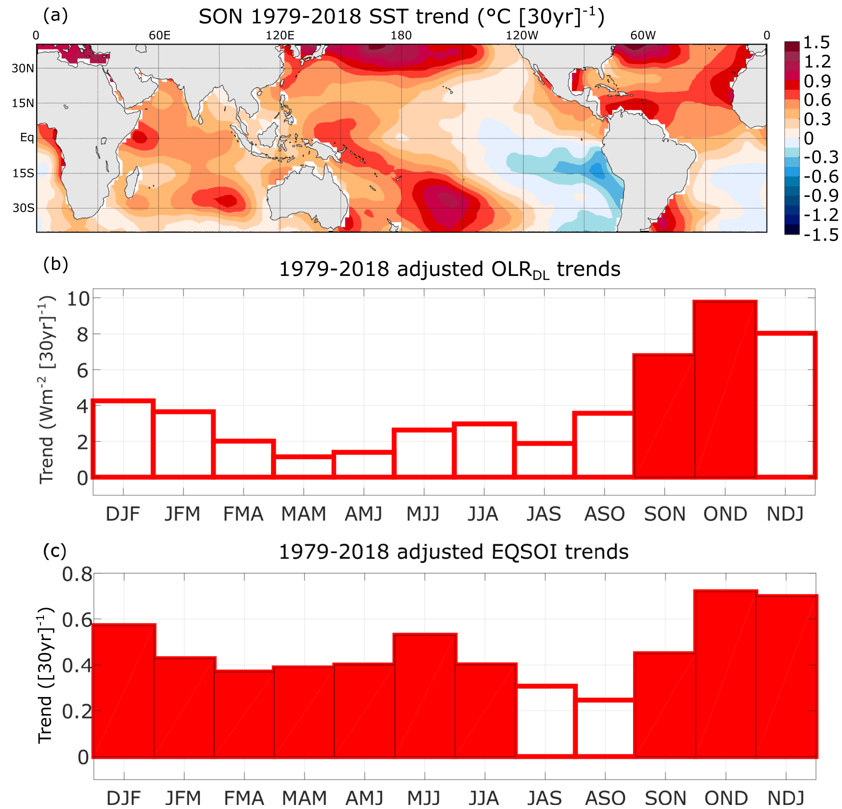

Figure 4. Tropical linear trends from 1979 to 2018. (a) The SON SSTA linear trend. (b) The seasonal linear trends of OLR_{DL} after linearly removing the influence of the Niño 3.4 index for each season. Filled bars indicate statistically significant trends at the 5% level according to the *F* test described in the text. (c) Same as in (b) but for the CDAS EQSOI.

gradient index captures, at least in part, the influence of a long-term trend. We elaborate on this observation in Figure 4, which shows linear trends of SST, Niño 3.4-adjusted OLR_{DL}, and Niño 3.4-adjusted EQSOI.

The 1979–2018 SON SST trend (Figure 4a) reveals enhanced warming in the western equatorial Pacific, particularly near Papua New Guinea, and reduced warming or cooling in the eastern equatorial Pacific, which is consistent with L'Heureux, Collins, et al. (2013). This SST trend pattern resembles the correlation pattern between Niño 3.4-adjusted SST and OLR_{DL} (Figure 2; uncentered pattern correlation (DelSole & Shukla, 2006) between Figures 2 and 4a is 0.76), although with differences in the location of the negative correlations/cooling east of the Date Line. Despite these differences, both patterns feature an enhanced zonal SST gradient between the western and central equatorial Pacific, which is expected to promote a tendency for the warm pool convection to remain anchored in the western equatorial Pacific. Therefore, the enhanced warming near Papua New Guinea and suppressed warming to the east over the past 40 years, especially in the second half of the period (Figure S3), have inhibited the eastward migration of the western Pacific warm pool that typically occurs when the Niño 3.4 index rises, supporting a speculation noted in McPhaden (2015). The impact of this SST trend is reflected in the Niño 3.4-adjusted OLR_{DL} trends (Figure 4b), which are positive in all seasons and statistically significant in SON and OND. Therefore, despite efforts to mitigate against the effects of longer-term trends in ENSO monitoring by modifying the Niño 3.4 index base period every five years, the effects of the OLR_{DL} trends cannot be neglected. Consistently, the Niño 3.4-adjusted CDAS EQSOI has undergone positive trends in all seasons (Figure 4c), indicating a strengthening of the Niño 3.4-independent Walker circulation. All trends are similar if Hadley Centre Sea Ice and SST version 1 data are used instead for all calculations (Figure S5), and the EQSOI trends are consistent in the Department of Energy Reanalysis 2 and ERA-Interim reanalysis but not the Climate Forecast System Reanalysis (see Text S2 and Figure S6). The negative Climate Forecast System Reanalysis EQSOI trends are likely spurious owing to an overly strong trade wind bias that was greatly reduced after 1998 (Xue et al., 2011), and so we conclude that the EQSOI trends derived from the other reanalyses are more reliable.

4. Conclusions

In this study, we address the absence of the expected boreal autumn tropical atmospheric conditions during recent borderline El Niño episodes, as in 2014 and 2018. We provide observational evidence that tropical SST patterns independent of the Niño 3.4 index, namely, the anomalous western/central Pacific zonal SST gradient, played a critical role in inhibiting the coupling between the atmosphere and the ocean during these events. Anomalous warming in the vicinity of Papua New Guinea inhibited the eastward migration of the eastern edge of the western Pacific warm pool that typically accompanies an elevated Niño 3.4 index, keeping the heaviest tropical rainfall anchored in the western Pacific rather than near the Date Line.

The positive deviations from the expected central Pacific OLR and the associated EQSOI during these recent events relate to a significant multidecadal trend of increasing central Pacific OLR and a strengthening Walker circulation, which is consistent with several recent studies (Hu et al., 2013; L'Heureux, Lee, et al., 2013; Sandeep et al., 2014; Seager et al., 2019; Sohn & Park, 2010; Solomon & Newman, 2012; Zhao & Allen, 2019) but inconsistent with the expected response to rising global temperatures from global climate models and through basic thermodynamic arguments (Held & Soden, 2006; Sohn et al., 2013; Vecchi et al., 2006). Given that this study is limited to a 40-year observational record, the reasons for this discrepancy are beyond the scope of this study (see, for example, Liu & Xie, 2018; Seager et al., 2019; Xie & Kosaka, 2017). Most relevant here, we find that a significant component of this trend in boreal autumn is independent of the Niño 3.4 index. This result is consistent with studies that have reported a pronounced Walker circulation strengthening after filtering out the influence of ENSO (L'Heureux, Lee, et al., 2013; Solomon & Newman, 2012). The implication is that the atmospheric response to typical El Niño (La Niña) SSTs has weakened (strengthened) over the past 40 years, based on a typical index for monitoring ENSO. This trend opposes the projected strengthened atmospheric response to El Niño with changing background SSTs under increasing greenhouse gases (Cai et al., 2014).

In this study, we focus on the atmospheric response to tropical SSTAs, holding the Niño 3.4 index fixed, but the zonal SST gradient pattern also may influence tropical SST evolution. For example, westerly wind events in the equatorial Pacific, an important forcing of ENSO (e.g., Vecchi & Harrison, 2000), are more likely to occur when the warm pool is extended eastward (Eisenman et al., 2005; Yu et al., 2003). Therefore, the increased zonal SST gradient during recent borderline El Niño events, which inhibited the eastward extension of the warm pool, potentially may have influenced the statistics of these stochastic wind events that regulated the tropical SST evolution, but this possibility requires additional study.

In addition, recent studies (Choi et al., 2011; Xiang et al., 2013) suggest that the change in mean state toward a stronger zonal SST gradient may be responsible for the more frequent occurrence of CP relative to EP El Niño. However, both EP and CP El Niño are expected to generate enhanced convection near the Date Line (e.g., Ashok et al., 2007; Santoso et al., 2019; Xiang et al., 2013), and so the modulating influence from the zonal SST gradient pattern (Figure 2) identified here is distinct from the influences described in those studies. This suggests that the zonal SST gradient pattern deserves attention separate from any of its potential influences on EP or CP ENSO. Given that ENSO's global impacts are driven by its effects on tropical convection, this SST gradient pattern may have important implications for ENSO teleconnection patterns, particularly in boreal fall (Bladé et al., 2008). These overall findings also confirm the utility of indexes that target the relationship between SST and tropical convection (L'Heureux et al., 2015; Williams & Patricola, 2018) to complement the Niño 3.4 index for monitoring ENSO.

To conclude, the delayed onset of the full coupling between atmosphere and ocean for the weak El Niño events of 2014/2015 and 2018/2019 may be rooted in a tropical SST pattern rather than internal atmospheric variability. The oceanic origins provide hope that these tropical atmospheric deviations from the canonical Niño 3.4 index relationships may be predictable on seasonal and possibly longer time scales, especially since the enhanced western Pacific zonal SST gradient is linked with a multidecadal trend. However, the ability of current dynamical or statistical forecast models to predict the Niño 3.4 index-independent component of this SST gradient pattern, and precisely how this gradient pattern may have impacted ENSO development, remain open questions.

Acknowledgments

We thank Xiaosong Yang, Tony Rosati, and two anonymous reviewers for their helpful comments that substantially improved the manuscript. N.C. Johnson was supported by awards NA14OAR4320106 and NA18OAR4320123 from the NOAA, U. S. Department of Commerce. C.-H. Chang was supported by National Research Foundation of Korea through grant NRF-2018R1A6A1A08025520. All data and code for this study are available online for download at https://figshare.com/projects/On_the_delayed_coupling_between_ocean_and_atmosphere_in_recent_weak_El_Ni_o_episodes/66935.

References

Ashok, K., Behera, S. K., Rao, S. A., Weng, H., & Yamagata, T. (2007). El Niño Modoki and its possible teleconnection. *Journal of Geophysical Research*, *112*, C11007. https://doi.org/10.1029/2006JC003798

Black, J., Johnson, N. C., Baxter, S., Feldstein, S. B., Harnos, D. S., & L'Heureux, M. L. (2017). The predictors and forecast skill of northern hemisphere teleconnection patterns for lead times of 3–4 weeks. *Monthly Weather Review*, *145*(7), 2855–2877. https://doi.org/10.1175/MWR-D-16-0394.1

Bladé, I., Newman, M., Alexander, M. A., & Scott, J. D. (2008). The late fall extratropical response to ENSO: Sensitivity to coupling and convection in the tropical west Pacific. *Journal of Climate*, *21*(23), 6101–6118. https://doi.org/10.1175/2008jcli1612.1

Cai, W., Borlace, S., Lengaigne, M., Van Rensch, P., Collins, M., Vecchi, G., et al. (2014). Increasing frequency of extreme El Niño events due to greenhouse warming. *Nature Climate Change*, *4*(2), 111–116. https://doi.org/10.1038/nclimate2100

Chiodi, A. M., & Harrison, D. E. (2013). El Niño impacts on seasonal U.S. atmospheric circulation, temperature, and precipitation anomalies: The OLR-event perspective. *Journal of Climate*, *26*(3), 822–837. https://doi.org/10.1175/JCLI-D-12-00097.1

Chiodi, A. M., & Harrison, D. E. (2017). Observed El Niño SSTA development and the effects of easterly and westerly wind events in 2014/15. *Journal of Climate*, *30*(4), 1505–1519. https://doi.org/10.1175/JCLI-D-16-0385.1

Choi, J., An, S.-I., Kug, J.-S., & Yeh, S.-W. (2011). The role of mean state on changes in El Niño's flavor. *Climate Dynamics*, *37*(5-6), 1205–1215. https://doi.org/10.1007/s00382-010-0912-1

Clarke, A. J. (2014). El Niño physics and El Niño predictability. *Annual Review of Marine Science*, *6*(1), 79–99. https://doi.org/10.1146/annurev-marine-010213-135026

Dee, D. P., Uppala, S. M., Simmons, A. J., Berrisford, P., Poli, P., Kobayashi, S., et al. (2011). The ERA-Interim reanalysis: Configuration and performance of the data assimilation system. *Quarterly Journal of the Royal Meteorological Society*, *137*(656), 553–597. https://doi.org/10.1002/qj.828

DelSole, T., & Shukla, J. (2006). Specification of wintertime North American surface temperature. *Journal of Climate*, *19*(12), 2691–2716. https://doi.org/10.1175/JCLI3704.1

Deser, C., & Wallace, J. M. (1990). Large-scale atmospheric circulation features of warm and cold episodes in the tropical Pacific. *Journal of Climate*, *3*(11), 1254–1281. https://doi.org/10.1175/1520-0442(1990)003<1254:LSACFO>2.0.CO;2

Eisenman, I., Yu, L., & Tziperman, E. (2005). Westerly wind bursts: ENSO's tail rather than the dog? *Journal of Climate*, *18*(24), 5224–5238. https://doi.org/10.1175/JCLI3588.1

Gill, A. E., & Rasmusson, E. M. (1983). The 1982–83 climate anomaly in the equatorial Pacific. *Nature*, *306*(5940), 229–234. https://doi.org/10.1038/306229a0

Held, I. M., & Soden, B. J. (2006). Robust responses of the hydrological cycle to global warming. *Journal of Climate*, *19*(21), 5686–5699. https://doi.org/10.1175/JCLI3990.1

Hu, S., & Fedorov, A. V. (2016). Exceptionally strong easterly wind burst stalling El Niño of 2014. *Proceedings of the National Academy of Sciences of the United States of America*, *113*(8), 2005–2010. https://doi.org/10.1073/pnas.1514182113

Hu, Z.-Z., Kumar, A., Ren, H., Wang, H., L'Heureux, M., & Jin, F. (2013). Weakened interannual variability in the tropical Pacific Ocean since 2000. *Journal of Climate*, *40*(11-12), 2745–2759. https://doi.org/10.1007/s00382-012-1431-z

Huang, B., Thorne, P. W., Banzon, V. F., Boyer, T., Chepurin, G., Lawrimore, J. H., et al. (2017). Extended Reconstructed Sea Surface Temperature, version 5 (ERSSTv5): Upgrades, validations, and intercomparisons. *Journal of Climate*, *30*(20), 8179–8205. https://doi.org/10.1175/JCLI-D-16-0836.1

Johnson, N. C., & Kosaka, Y. (2016). The impact of eastern equatorial Pacific convection on the diversity of boreal winter El Niño teleconnection patterns. *Climate Dynamics*, *47*(12), 3737–3765. https://doi.org/10.1007/s00382-016-3039-1

Kalnay, E., Kanamitsu, M., Kistler, R., Collins, W., Deaven, D., Gandin, L., et al. (1996). The NCEP/NCAR 40-Year reanalysis project. *Bulletin of the American Meteorological Society*, *77*(3), 437–471. https://doi.org/10.1175/1520-0477(1996)077<0437:TNYRP>2.0.CO;2

Kanamitsu, M., Ebisuzaki, W., Woolen, J., Yang, S.-K., Hnilo, J. J., Fiorino, M., & Potter, G. L. (2002). NCEP-DOE AMIP-II Reanalysis (R-2). *Bulletin of the American Meteorological Society*, *83*(11), 1631–1644. https://doi.org/10.1175/BAMS-83-11-1631

Lee, H.-T., Gruber, A., Ellingson, R. G., & Laszlo, I. (2007). Development of the HIRS outgoing longwave radiation climate dataset. *Journal of Atmospheric and Oceanic Technology*, *24*(12), 2029–2047. https://doi.org/0.1175/2007JTECHA989.1, https://doi.org/10.1175/2007JTECHA989.1

Levine, A. F. Z., & McPhaden, M. J. (2016). How the July 2014 easterly wind burst gave the 2015–2016 El Niño a head start. *Geophysical Research Letters*, *43*, 6503–6510. https://doi.org/10.1002/2016GL069204

L'Heureux, M., Collins, D., & Hu, Z.-Z. (2013). Linear trends in sea surface temperature of the tropical Pacific Ocean and implications for the El Niño-Southern Oscillation. *Climate Dynamics*, *40*(5-6), 1223–1236. https://doi.org/10.1007/s00382-012-1331-2

L'Heureux, M. L., Lee, S., & Lyon, B. (2013). Recent multidecadal strengthening of the Walker circulation across the tropical Pacific. *Nature Climate Change*, *3*, 571–576. https://doi.org/10.1038/nclimate1840

L'Heureux, M. L., Tippett, M. K., & Barnston, A. G. (2015). Characterizing ENSO coupled variability and its impact on North American seasonal precipitation and temperature. *Journal of Climate*, *28*(10), 4231–4245. https://doi.org/10.1175/JCLI-D-14-00508.1

Liu, W., & Xie, S. P. (2018). An ocean view of the global surface warming hiatus. *Oceanography*, *31*(2), 72–79. https://doi.org/10.5670/oceanog.2018.217

McPhaden, M. J. (2015). Playing hide and seek with El Niño. *Nature Climate Change*, *5*(9), 791–795. https://doi.org/10.1038/nclimate2775

Menkes, C. E., Lengaigne, M., Vialard, J., Puy, M., Marchesiello, P., Cravatte, S., & Cambon, G. (2014). About the role of westerly wind events in the possible development of an El Niño in 2014. *Geophysical Research Letters*, *41*, 6476–6483. https://doi.org/10.1002/2014GL061186

Rayner, N. A., Parker, D. E., Horton, E. B., Folland, C. K., Alexander, L. V., Rowell, D. P., et al. (2003). Global analyses of sea surface temperature, sea ice, and night marine air temperature since the late nineteenth century. *Journal of Geophysical Research*, *108*(D14), 4407. https://doi.org/10.1029/2002JD002670

Saha, S., Moorthi, S., Pan, H.-L., Wu, X., Wang, J., Nadiga, S., et al. (2010). The NCEP Climate Forecast System Reanalysis. *Bulletin of the American Meteorological Society*, *91*(8), 1015–1058. https://doi.org/10.1175/2010BAMS3001.1

Sandeep, S., Stordal, F., Sardeshmukh, P. D., & Compo, G. P. (2014). Pacific Walker circulation variability in coupled and uncoupled climate models. *Climate Dynamics*, *43*(1-2), 103–117. https://doi.org/10.1007/s00382-014-2135-3

Santer, B. D., Wigley, T. M. L., Boyle, J. S., Gaffen, D. J., Hnilo, J. J., Nychka, D., & Taylor, K. E. (2000). Statistical significance of trends and trend differences in layer-average atmospheric temperature time series. *Journal of Geophysical Research*, *105*(D6), 7337–7356. https://doi.org/10.1029/1999JD901105

Santoso, A., Hendon, H., Watkins, A., Power, S., Dommenget, D., England, M., et al. (2019). Dynamics and predictability of El Niño-Southern Oscillation: An Australian perspective on progress and challenges. *Bulletin of the American Meteorological Society*, *100*(3), 403–420. https://doi.org/10.1175/BAMS-D-18-0057.1

Seager, R., Cane, M., Henderson, N., Lee, D.-E., Abernathy, R., & Zhang, H. (2019). Strengthening tropical Pacific zonal sea surface temperature gradient consistent with rising greenhouse gases. *Nature Climate Change*, *9*(7), 517–522. https://doi.org/10.1038/s41558-019-0505-x

Shu, L., & Clarke, A. J. (2002). Using an ocean model to examine ENSO dynamics. *Journal of Physical Oceanography*, *32*(3), 903–923. https://doi.org/10.1175/1520-0485(2002)032<0903:UAOMTE>2.0.CO;2

Smoliak, B. V., Wallace, J. M., Stoelinga, M. T., & Mitchell, T. P. (2010). Applications of partial least squares regression to the diagnosis of year-to-year variations in Pacific Northwest snowpack and Atlantic hurricanes. *Geophysical Research Letters*, *37*, L03801. https://doi.org/10.1029/2009GL041478

Sohn, B. J., & Park, S.-C. (2010). Strengthened tropical circulations in past three decades inferred from water vapor transport. *Journal of Geophysical Research*, *115*, D15112. https://doi.org/10.1029/2009JD013713

Sohn, B. J., Yeh, S.-W., Schmetz, J., & Song, H.-J. (2013). Observational evidences of Walker circulation change over the last 30 years contrasting with GCM results. *Climate Dynamics*, *40*(7-8), 1721–1732. https://doi.org/10.1007/s00382-012-1484-z

Solomon, A., & Newman, M. (2012). Reconciling disparate twentieth century Indo-Pacific ocean temperature trends in the instrumental record. *Nature Climate Change*, *2*(9), 691–699. https://doi.org/10.1038/nclimate159

Takahashi, K., Montecinos, A., Goubanova, K., & Dewitte, B. (2011). ENSO regimes: Reinterpreting the canonical and Modoki El Niño. *Geophysical Research Letters*, *38*, L10704. https://doi.org/10.1029/2011GL047364

Trenberth, K. E., Branstator, G. W., Karoly, D., Kumar, A., Lau, N. C., & Ropelewski, C. (1998). Progress during TOGA in understanding and modeling global teleconnections associated with tropical sea surface temperatures. *Journal of Geophysical Research*, *103*(C7), 14,291–14,324. https://doi.org/10.1029/97JC01444

Vecchi, G. A., & Harrison, D. E. (2000). Tropical Pacific sea surface temperature anomalies, El Niño, and equatorial westerly wind events. *Journal of Climate*, *13*, 1814–1830. https://doi.org/10.1175/1520-0442%282000%29013<1814%3ATPSSTA>2.0.CO%3B2

Vecchi, G. A., Soden, B. J., Wittenberg, A. T., Held, I. M., Leetmaa, A., & Harrison, M. J. (2006). Weakening of tropical Pacific atmospheric circulation due to anthropogenic forcing. *Nature*, *441*(7089), 73–76. https://doi.org/10.1038/nature04744

Williams, I. N., & Patricola, C. M. (2018). Diversity of ENSO events unified by convective threshold sea surface temperature: A nonlinear ENSO index. *Geophysical Research Letters*, *45*, 9236–9244. https://doi.org/10.1029/2018GL079203

Wold, H. (1966). Estimation of principal components and related models by iterative least squares. In P. R. Krishnaiah (Ed.), *Multivariate analysis* (pp. 391–420). New York: Academic.

Xiang, B., Wang, B., & Li, T. (2013). A new paradigm for the predominance of standing central Pacific warming after the late 1990s. *Climate Dynamics*, *41*(2), 327–340. https://doi.org/10.1007/s00382-012-1427-8

Xie, S.-P., & Kosaka, Y. (2017). What caused the global surface warming hiatus of 1998–2013? *Current Climate Change Reports*, *3*(2), 128–140. https://doi.org/10.1007/s40641-017-0063-0

Xue, Y., Huang, B., Hu, Z.-Z., Kumar, A., Wen, C., Behringer, D., & Nadiga, S. (2011). An assessment of oceanic variability in the NCEP Climate Forecast System Reanalysis. *Climate Dynamics*, *37*(11-12), 2511–2539. https://doi.org/10.1007/s00382-010-0954-4

Yu, J.-Y., & Kao, H.-Y. (2007). Decadal changes of ENSO persistence barrier in SST and ocean heat content indices: 1958–2001. *Journal of Geophysical Research*, *112*, D13106. https://doi.org/10.1029/2006JD007654

Yu, L., Weller, R. A., & Liu, W. T. (2003). Case analysis of a role of ENSO in regulating the generation of westerly wind bursts in the western equatorial Pacific. *Journal of Geophysical Research*, *108*(C4), 3128. https://doi.org/10.1029/2002JC001498

Zhao, X., & Allen, R. J. (2019). Strengthening of the Walker circulation in recent decades and the role of natural sea surface temperature variability. *Environmental Research Communications*, *1*(2), 021003. https://doi.org/10.1088/2515-7620/ab0dab